

Input-Output Pairing Selection of Three-Input Integrated Dc-Dc Converter Based on Gramian Analysis

MANOGNA M, AMARENDRA REDDY B, PADMA KOTTALA

Department of Electrical Engineering
Andhra University College of Engineering
Visakhapatnam, Andhra Pradesh
INDIA

Abstract: - Because of its integrated structure and the presence of common parts, the Three-Input Integrated Dc-Dc (TIID) Converter creates interactions between its three regulated output variables, making control challenging. Therefore, it is essential to quantify the interactions in advance to comprehend the converter's behavior and create the controller for an integrated three-input dc-dc converter. This quantification aids in solving the integrated converter's pairing issue. Both frequency-based and dc gain-based interaction measurements are used to quantify the interactions of integrated dc-dc converters. This work investigates frequency-based (Gramian) interactions and their computational process, whereby the input-output pairing is determined. These include the H_2 -norm ($H_2 - n$) Interaction Array, Hankel Interaction Index Array (HIIA) and Participation Matrix (PM). The effects of altering the TIID converter's parameters and operating conditions on these interactions are analyzed and depicted graphically. A 400 W TIID converter operating at 24V, 30V, 36V and 48V is considered in order to measure these interactions.

Key-Words: Multi-input converter, Integrated dc-dc converter, Three-input integrated dc-dc converter, interaction measures, Gramian Interaction Measures, Hankel Interaction Index Array, Participation Matrix, H_2 - norm Interaction Array

Received: July 13, 2022. Revised: March 23, 2023. Accepted: April 24, 2023. Published: July 3, 2023.

1 Introduction

Switched mode power systems are by nature Multi-input Multi-output (MIMO), needing control over one or more variables to enable flexible operation and efficient use of a range of sources. Because each input signal may have an effect on many controlled variable output signals, these systems include interactions between the input/output loops. This class comprises dc-dc converters with multiple inputs. Dual-input and three-input dc-dc converters include multiple energy store elements (ranging from 2 to n) [1]. The behavior of these elements varies depending on the mode, processing stored energy in a different fashion. The interactions between inputs and outputs are caused by this nature. Other elements that also influence interactions are as follows: (i) The rate at which energy is stored and released by the inductive and capacitive elements in different circuit sections; (ii) The duration of overlaps between different sources feeding different circuit sections; (iii) The duty ratio and relative phase position of each switching device; and (iv) Changes in the circuit configuration caused by different switching cycle operating modes. Because of this, controlling

multivariable systems is usually far more challenging than controlling a single-input, single-output system. Therefore, it's critical to measure the level of interaction in order to choose the right input/output (i/o) pairing and prevent instability in the control loops while minimizing interactions. Thus, depending on the i/o pairing, a control structure such as centralized control or decoupled control, decentralized control [2] can be selected. Thus, in order to design a suitable controller. Therefore, in order to create an appropriate controller for MIMO converters, interactions must be described.

The literature has reported on a number of techniques for locating and measuring the control loop interactions [3]. These are divided into two categories: (a) Interactions based on DC gain and (b) interactions based on non-DC gain. DC-gain based interaction measurements are input-output interaction measurements that are based on the steady-state matrix or dc-gain of the system. This group includes Neiderlenski's index (NI) and the relative gain array (RGA) [4]. Two additional categories for the non-dc-gain based interaction metrics are specific frequency

range (SFR) based interactions and whole frequency range (EFR) based interactions. Effective RGA and RGA number ($RGAN$) are SFR based interactions. The Gramian-based interactions are a type of EFR-based interaction [5]. Examples of Gramian-based interactions that have been reported in the literature include the participation matrix (PM), Hankel Interaction Index Array ($HIIA$) and H_2 -norm ($H_2 - n$) based interactions [6].

Novelty of the paper:

A fourth-order, three-input integrated dc-dc converter circuit is shown in Fig 1. To make a TIID converter just integrate two Boost converters and a Buck-Boost converter using the methods outlined in [7]. By monitoring the input currents of two separate sources along with output voltage, the converter is treated as a three input-three output converter. Therefore, this work's contribution is the formulation of a dc-dc converter with three inputs and three outputs, as well as the use of an average state-space model to represent the converter. The whole interaction study is carried out from a multivariable perspective using this model. Gramian-based metrics are used to systematically quantify the interactions of the TIID converter. Therefore, an analysis of the integrated converter's interactions under parameter modifications [8–13] is attempted in this article. The effect of parameter changes on quantifications are graphically depicted. Gramian based analysis plays crucial role in determining the impact of inputs on output so as to determine the type of controller for the converter systems [14-16]. The suggested controller is yet to be designed for TIID converter. This converter finds applications in renewable energy based Electric Vehicles [17], Microgrid systems [18],[19]. The Controller suggested by this Gramian analysis can be designed using different available methods like adaptive Participation Matrix based H_∞ control [20], Optimal multivariable control [21] and online tuning control methodology [22].

The paper is divided into the following sessions: (i) mathematical modeling of the TIID Converter, (ii) quantifying the above interactions while considering the TIID converter and identifying i/o pairing through Interaction Metrics (IMs), (iii) computing IMs under different operating conditions, (iv) illustrating the impact of parameter variation through IMs, and finalizing the choice of controller type for the TIID converter based on the i/o pairing suggested by IMs, (v) the real time results are shown followed by Conclusions.

2 Modeling of TIID Converter

In Fig. 1, the converter for TIID is shown. For this integrated converter, three distinct voltage sources (V_{g1} , V_{g2} and V_{g3}) are suggested. Furthermore, for proper load sharing and power continuity, the output voltage V_o and the LVS currents (i_{g1} and i_{g2} which are the input currents of V_{g1} , V_{g2} and V_{g3}) are regulated. Three duty ratio control signals d_1 , d_2 and d_3 are used in the proposed converter to independently regulate each of the three switches. As a result, three different sources of power can supply the load simultaneously or separately. The duty ratios function as the governing inputs of the converter. This enables four different modes of operation to be possible as shown in fig 2. As a result, each mode of operation's state space equations evaluates the converter's dynamics and performance. The input and output variables are hence functionally dependent on one another. Hence, this functional dependency is modelled by a set of transfer functions assembled in TFM form. To derive the TFM, state-variable model along with small-signal modelling is implemented in all the operating modes.

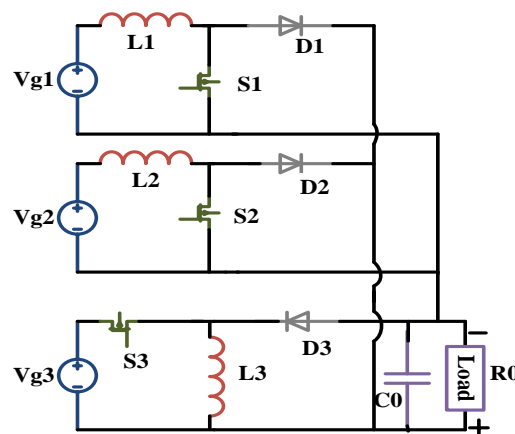


Fig. 1. Circuit diagram of the TIID converter

Eqs (1), (2) give the state-space equations for the four operational modes, where $i=1,2,3,4$. The small-signal modelling of the converter can be generated by averaging these state equations as indicated in (3) and applying minor change \hat{k} to each of the state variables as indicated in (4). From there, the TFM G as indicated in (5) is developed in a MATLAB environment. The detailed modelling is given in [23].

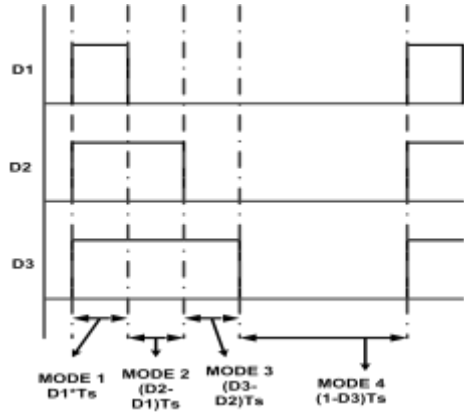


Fig.2. PWM gating signals for the TIID Converter

$$\dot{x} = A_i x + B_i u, \quad y = E_{0i} x + F_{0i} u \quad (1)$$

$$y = \begin{bmatrix} v_0 \\ i_{g1} \\ i_{g2} \end{bmatrix} E_{0i} = \begin{bmatrix} E_1 \\ P_{1i} \\ P_{2i} \end{bmatrix} F_{0i} = \begin{bmatrix} F_1 \\ F_{1i} \\ F_{2i} \end{bmatrix} \quad (2)$$

$$\begin{bmatrix} A \\ B \\ E \\ F \end{bmatrix} = \begin{bmatrix} d_1 A_1 + (d_2 - d_1) A_2 + (d_3 - d_2) A_3 + (1 - d_3) A_4 \\ d_1 B_1 + (d_2 - d_1) B_2 + (d_3 - d_2) B_3 + (1 - d_3) B_4 \\ d_1 E_1 + (d_2 - d_1) E_2 + (d_3 - d_2) E_3 + (1 - d_3) E_4 \\ d_1 F_1 + (d_2 - d_1) F_2 + (d_3 - d_2) F_3 + (1 - d_3) F_4 \end{bmatrix} \quad (3)$$

$$x(t) = X + \hat{x}, \quad u(t) = U + \hat{u}, \quad y(t) = Y + \hat{y}, \quad d_1 = D_1 + \hat{d}_1, \quad d_2 = D_2 + \hat{d}_2, \quad d_3 = D_3 + \hat{d}_3, \quad (1 - d_3) = D_3^1 - \hat{d}_3 \quad (4)$$

$$\begin{bmatrix} \hat{v}_0(s) \\ \hat{i}_{g1}(s) \\ \hat{i}_{g2}(s) \end{bmatrix} = \begin{bmatrix} G_{11}(s) & G_{12}(s) & G_{13}(s) \\ G_{21}(s) & G_{22}(s) & G_{23}(s) \\ G_{31}(s) & G_{32}(s) & G_{33}(s) \end{bmatrix} \begin{bmatrix} \hat{d}_1(s) \\ \hat{d}_2(s) \\ \hat{d}_3(s) \end{bmatrix} \quad (5)$$

$$G = \begin{bmatrix} G_{11}(s) & G_{12}(s) & G_{13}(s) \\ G_{21}(s) & G_{22}(s) & G_{23}(s) \\ G_{31}(s) & G_{32}(s) & G_{33}(s) \end{bmatrix} \quad (6)$$

3. Interaction Measures of the Converter

The TFM obtained in section 2 is used to quantify the interactions of the TIID converter. There are two categories to detect and measure the control-loop interactions: (a) dc-gain based interactions, and (b) non-dc-gain based interactions. The classification of interaction measures is listed in Figure 7, and only Gramian Interaction Metrics (GIMs) are used for the quantification of the TIID converter's interactions in this research.

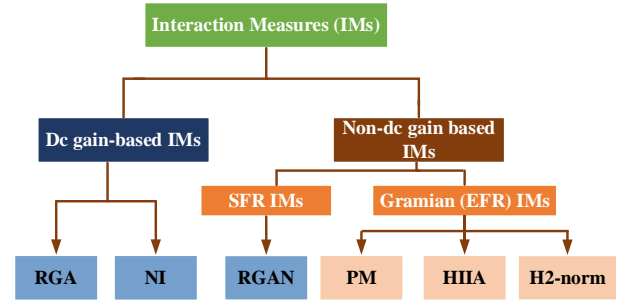


Fig.3. Classification of IMs used in analysis of TIID Converter.

3.1 Gramian measures:

The basis for the Gramian measures is the controllability Gramian W_c and observability Gramian W_o of each converter subsystem, which are defined as (8) satisfies equation (7). H_2 -norm based interactions, PM and $HIIA$ are a few of the EFR [8] metrics discussed in this work.

$$\begin{aligned} A W_c + W_c A^T + B B^T &= 0 \\ A^T W_o + W_o A + C^T C &= 0 \end{aligned} \quad (7)$$

$$W_c = \int_0^{\infty} e^{A t} B B^T e^{A^T t} dt, \quad W_o = \int_0^{\infty} e^{A^T t} C^T C e^{A t} dt \quad (8)$$

3.1.1 Hankel Interaction Index Array (HIIA):

Using the Hankel Singular Value (HSV), (7) is utilized to find the Hankel norm of each subsystem of G . The Hankel norm of each subsystem of a three-variable system is organized as a matrix, normalized to produce $HIIA$, and then provided as (9) and (10).

$$\|G\|_H = \sqrt{\sigma_{\max}(W_c W_o)} \quad (9)$$

$$[\Sigma H]_{ij} = \frac{\|G_{ij}\|_H}{\sum_{kl} \|G_{kl}\|_H} \quad (10)$$

The pairing in HIIA IM is done as follows: The largest element in the matrix should be found first, followed by the elimination of the row and column that correspond to it. Next, the associated input and output for this element should be paired. After that, choose the element that is second highest and match its input to output. The last element's input and output are matched.

The Hankel norm, or maximum of HSVs, is the basis for the $HIIA$; if certain HSVs are near the maximum HSV, their significance is not taken into account during computation. This restriction is addressed by PM , which takes W_c and W_o traces into account.

3.1.2 Participation matrix (PM):

Equation (11) is used in the definition of PM. In this case, $tr(W_{cj}W_{oi})$ represents the trace of the subsystem G_{ij} , and $tr(W_cW_o)$ represents the converter's trace that is, the total of the traces of the nine subsystems. The PM IM pairing rule is the same as the HIIA.

$$[\Phi]_{ij} = \frac{tr(W_{cj}W_{oi})}{tr(W_cW_o)} \quad (11)$$

3.1.3 H₂-norm based interactions(H₂-norm):

Similar to HIIA, the H₂-norm based interaction takes into account the H₂-norm, which is given as (12). To produce the -norm interaction as in (13), the H₂ -norm of each sub-system is computed, arranged in a matrix, and normalized. The -norm can be calculated in two different ways: (i) using B and W_o , (ii) using C and W_c . The H₂-norm IM pairing rule is the same as the HIIA.

$$\|G\|_2 = \sqrt{tr(B^T W_o B)} = \sqrt{tr(C W_c C^T)} \quad (12)$$

$$[\Sigma H]_{ij} = \frac{\|G_{ij}\|_H}{\sum_{kl} \|G_{kl}\|_H} \quad (13)$$

Table 1. Gramian IMs of TIID Converter

S.no	IMs	Matrix	Pairing
1	HIIA	$\begin{bmatrix} 0.0288 & 0.1099 & 0.0145 \\ 0.1348 & 0.1878 & 0.1309 \\ 0.1499 & 0.0880 & 0.1553 \end{bmatrix}$	Diagonal pairing
2	PM	$\begin{bmatrix} 0.0062 & 0.1047 & 0.0019 \\ 0.1491 & 0.1492 & 0.1620 \\ 0.1667 & 0.0337 & 0.2265 \end{bmatrix}$	Diagonal pairing
3	H ₂ - n	$\begin{bmatrix} 0.0484 & 0.1842 & 0.0242 \\ 0.1289 & 0.2105 & 0.0897 \\ 0.0918 & 0.0970 & 0.1253 \end{bmatrix}$	Diagonal pairing

The TFM of the TIID converter G is obtained in MATLAB environment as given in Appendix (A1) - (A9). These are used to find the GIMs of TIID converter and are given in Table 1. Take a look at the HIIA Matrix in Table 1. The greatest magnitude element in this instance is 0.1878, and it is located at (2,2). Hence, the identification of the second controlling signal comes from the second row and second column. Pair it with the second controlled

output, i.e., $d_2 - i_{g2}$. Then, identifying method will prevent pairing d_2 with i_{g2} and V_o . Identification from the second row and second column is satisfied in this instance. Next, locate element 0.1553, which has the second largest magnitude. This can be found by going from the third row to the third column. This implies the combination of $d_3 - i_{g3}$. Thus, throw out the second and third columns and the rows. Obviously, the first output and the first input should be coupled i.e., $d_1 - V_o$. Thus, suggesting diagonal pairing of inputs and outputs. Similarly, the other two measures also suggest the same pairing. The block diagram in Fig. 4 illustrates the suggested diagonal controller structure for this converter system, which is based on the diagonal elements' greater dominance than the others.

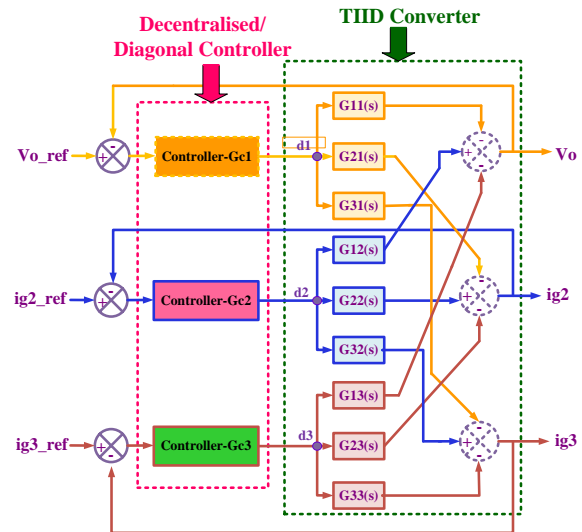


Fig.4. De-centralised control structure for TIID converter.

4. Interaction Measures for Different Operating Conditions:

Various perturbed situations are taken into account, and the interaction matrices are calculated for each potential scenario. A maximum fluctuation in load resistance of $\pm 50\%$ and a maximum variation in source voltage of $\pm 20\%$ are considered. Table 2 tabulates the interaction matrices for nominal values and under perturbed conditions. Table 2 shows that each situation's pairing recommendation is the same as in the nominal example.

5. Impact of Parameter Variation on Interaction Measures:

Plotting of the impact of parameter changes on the diagonal parts of the interaction matrix is done separately. This figure aids in the analysis of the interactions caused by parameter changes and identifies the crucial parameters that affect the processing of converter power. The impact of interactions is to be known when there is a fluctuation of $\pm 20\%$ in parameters L_1, L_2, L_3 and C_o .

5.1. Variation of R versus elements of IMs:

To observe how variations in load resistance (R) affect interactions, the load resistance is adjusted by $\pm 50\%$. A graphic representation of each parameter's impact on the interaction measures ($HIIA, PM$ and $H_2 - n$) is provided. These can be seen from Fig. 5- Fig. 7. The numbers show that a few of the interaction parts vary slightly from one another. The diagonal IO-pairing is suggested by this graphical illustration. Although there is a small difference in the diagonal elements of PM , it has no bearing on the matching recommendation. Therefore, it may be said that parameter modification has no effect on the interaction measurements.

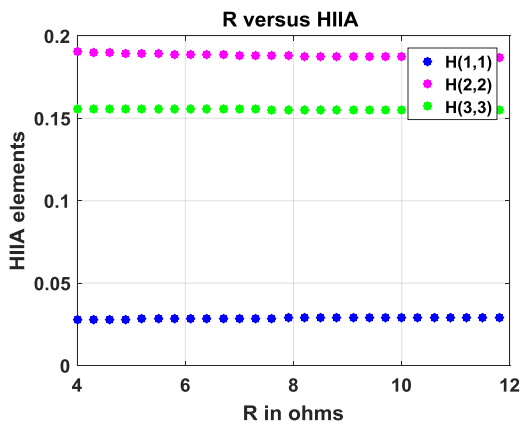


Fig. 5. R vs $HIIA$'s diagonal elements

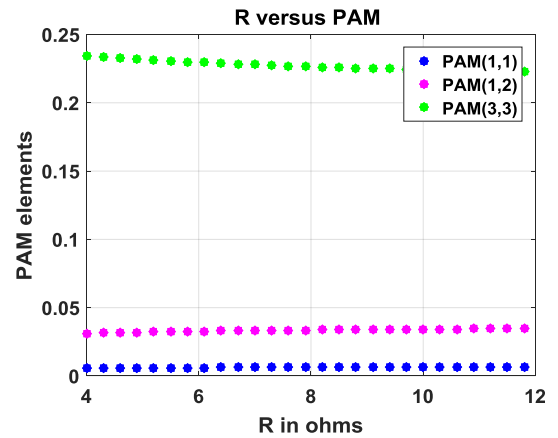


Fig. 6. R vs PM 's diagonal elements

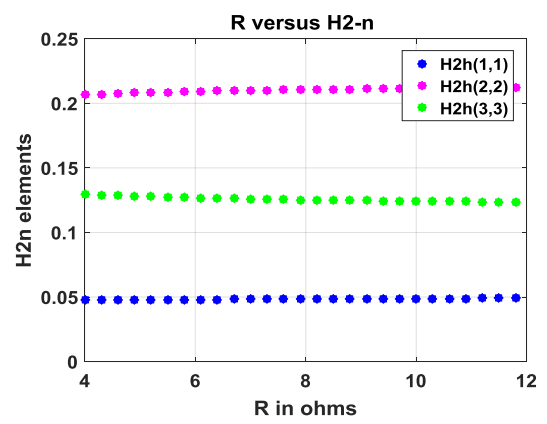


Fig. 7. R vs $H_2 - n$'s diagonal elements

5.2. L_1 variation in relation to interaction matrix elements:

L_1 variation, which is varied by $\pm 20\%$, is taken into consideration to examine how it affects interactions. In Figs. 8-10, the effects of each parameter on the interaction measures are visually displayed.

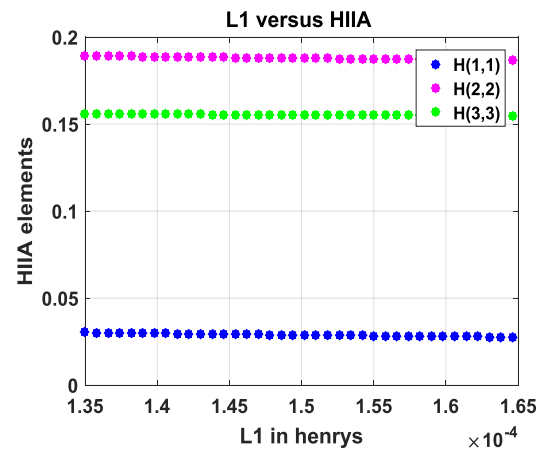


Fig. 8. L_1 vs $HIIA$'s diagonal elements

Table 2. GIMs of TIID Converter at different operating conditions

Parameters	HIIA	PM	H ₂ -norm
$V_{g1} = 42$ (20%)	$\begin{bmatrix} 0.0372 & 0.0990 & 0.0232 \\ 0.1416 & 0.1710 & 0.1364 \\ 0.1548 & 0.0783 & 0.1585 \end{bmatrix}$	$\begin{bmatrix} 0.0171 & 0.0923 & 0.0049 \\ 0.1678 & 0.1297 & 0.1700 \\ 0.1684 & 0.0294 & 0.2204 \end{bmatrix}$	$\begin{bmatrix} 0.0714 & 0.1662 & 0.0475 \\ 0.1479 & 0.1881 & 0.0989 \\ 0.0855 & 0.0867 & 0.1078 \end{bmatrix}$
$V_{g1} = 30$	$\begin{bmatrix} 0.0398 & 0.1187 & 0.0417 \\ 0.1143 & 0.1978 & 0.1163 \\ 0.1344 & 0.0956 & 0.1415 \end{bmatrix}$	$\begin{bmatrix} 0.0159 & 0.1181 & 0.0245 \\ 0.1217 & 0.1670 & 0.1506 \\ 0.1495 & 0.0375 & 0.2150 \end{bmatrix}$	$\begin{bmatrix} 0.0851 & 0.1665 & 0.0861 \\ 0.0850 & 0.1898 & 0.0912 \\ 0.0851 & 0.0875 & 0.1237 \end{bmatrix}$
$V_{g2} = 36$	$\begin{bmatrix} 0.0344 & 0.1134 & 0.0433 \\ 0.1205 & 0.1943 & 0.1192 \\ 0.1391 & 0.0907 & 0.1452 \end{bmatrix}$	$\begin{bmatrix} 0.0106 & 0.1183 & 0.0250 \\ 0.1246 & 0.1684 & 0.1499 \\ 0.1515 & 0.0380 & 0.2138 \end{bmatrix}$	$\begin{bmatrix} 0.0699 & 0.1719 & 0.0867 \\ 0.0877 & 0.1963 & 0.0912 \\ 0.0827 & 0.0904 & 0.1233 \end{bmatrix}$
$V_{g2} = 25$	$\begin{bmatrix} 0.0356 & 0.1012 & 0.0271 \\ 0.1384 & 0.1726 & 0.1357 \\ 0.1515 & 0.0811 & 0.1569 \end{bmatrix}$	$\begin{bmatrix} 0.0158 & 0.0881 & 0.0072 \\ 0.1663 & 0.1256 & 0.1762 \\ 0.1685 & 0.0283 & 0.2239 \end{bmatrix}$	$\begin{bmatrix} 0.0689 & 0.1595 & 0.0579 \\ 0.1470 & 0.1824 & 0.1056 \\ 0.0862 & 0.0841 & 0.1083 \end{bmatrix}$
$V_{g3} = 28$	$\begin{bmatrix} 0.0275 & 0.1149 & 0.0141 \\ 0.1306 & 0.1918 & 0.1292 \\ 0.1461 & 0.0926 & 0.1532 \end{bmatrix}$	$\begin{bmatrix} 0.0055 & 0.1054 & 0.0018 \\ 0.1448 & 0.1492 & 0.1645 \\ 0.1657 & 0.0335 & 0.2296 \end{bmatrix}$	$\begin{bmatrix} 0.0506 & 0.1826 & 0.0241 \\ 0.1240 & 0.2084 & 0.0922 \\ 0.0942 & 0.0960 & 0.1279 \end{bmatrix}$
$V_{g3} = 20$	$\begin{bmatrix} 0.0308 & 0.1057 & 0.0149 \\ 0.1390 & 0.1829 & 0.1325 \\ 0.1538 & 0.0832 & 0.1573 \end{bmatrix}$	$\begin{bmatrix} 0.0078 & 0.1075 & 0.0020 \\ 0.1526 & 0.1502 & 0.1581 \\ 0.1662 & 0.0340 & 0.2215 \end{bmatrix}$	$\begin{bmatrix} 0.0502 & 0.1878 & 0.0241 \\ 0.1323 & 0.2116 & 0.0864 \\ 0.0887 & 0.0976 & 0.1212 \end{bmatrix}$
$R = 4$	$\begin{bmatrix} 0.0278 & 0.0992 & 0.0133 \\ 0.1391 & 0.1905 & 0.1316 \\ 0.1522 & 0.0909 & 0.1555 \end{bmatrix}$	$\begin{bmatrix} 0.0060 & 0.0788 & 0.0016 \\ 0.1644 & 0.1400 & 0.1684 \\ 0.1755 & 0.0312 & 0.2340 \end{bmatrix}$	$\begin{bmatrix} 0.0480 & 0.1712 & 0.0231 \\ 0.1407 & 0.2065 & 0.0920 \\ 0.0943 & 0.0947 & 0.1297 \end{bmatrix}$
$R = 12$ (50%)	$\begin{bmatrix} 0.0294 & 0.1142 & 0.0150 \\ 0.1333 & 0.1867 & 0.1306 \\ 0.1490 & 0.0869 & 0.1551 \end{bmatrix}$	$\begin{bmatrix} 0.0064 & 0.1161 & 0.0020 \\ 0.1435 & 0.1531 & 0.1589 \\ 0.1627 & 0.0347 & 0.2226 \end{bmatrix}$	$\begin{bmatrix} 0.0490 & 0.1889 & 0.0246 \\ 0.1247 & 0.2119 & 0.0888 \\ 0.0908 & 0.0978 & 0.1235 \end{bmatrix}$

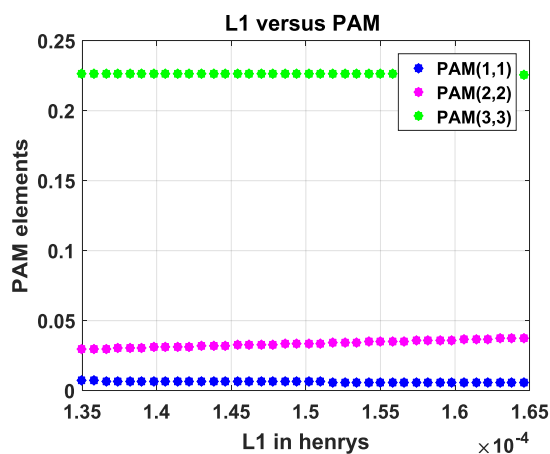


Fig. 9. L_1 vs PM 's diagonal elements

5.3. L_2 variation in relation to interaction matrix elements:

L_2 variation, which is varied by $\pm 20\%$, is taken into consideration to examine how it affects interactions. In Figs. 11-13, the effects of each parameter on the interaction measures are visually displayed.

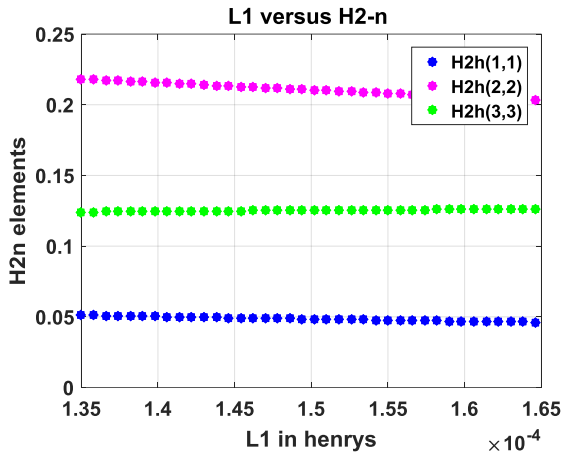


Fig. 10. L_1 vs $H_2 - n$'s diagonal elements

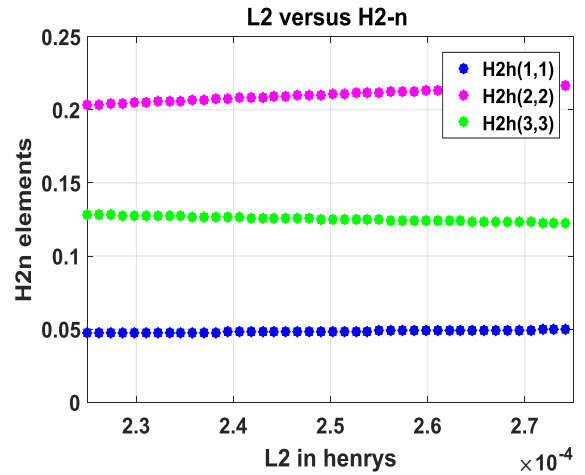


Fig. 13. L_2 vs $H_2 - n$'s diagonal elements.

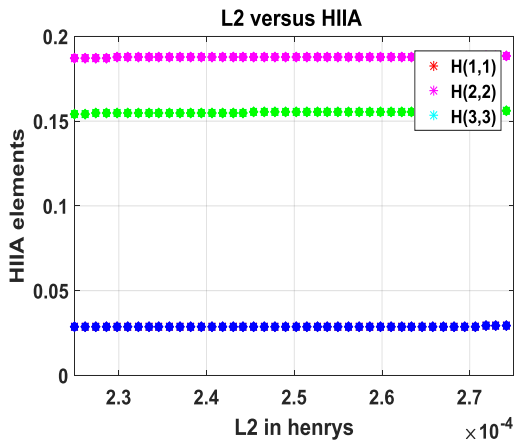


Fig. 11. L_2 vs $HIIA$'s diagonal elements

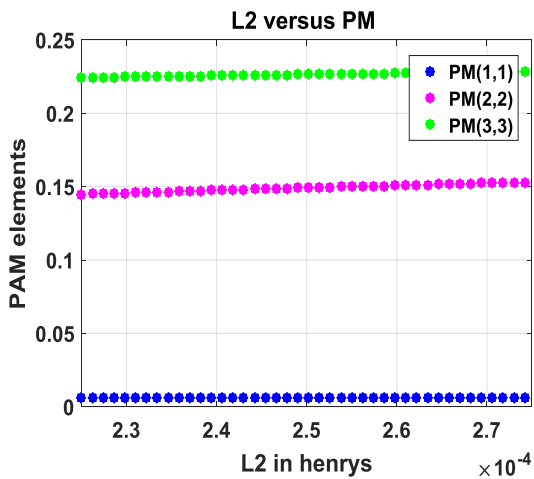


Fig. 12. L_2 vs PM 's diagonal elements.

5.4. L_3 variation in relation to interaction matrix elements:

L_3 variation, which is varied by $\pm 20\%$, is taken into consideration to examine how it affects interactions. In Figs. 14-16, the effects of each parameter on the interaction measures are visually displayed.

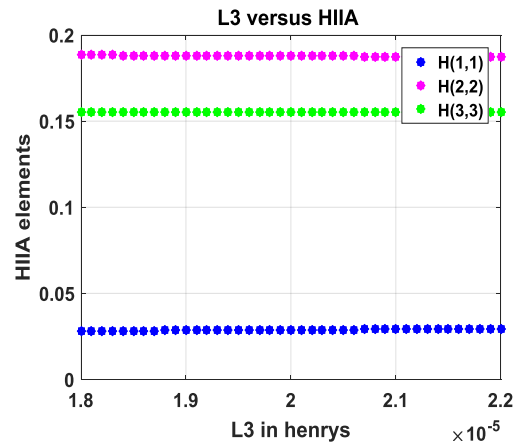


Fig. 14. L_3 vs $HIIA$'s diagonal elements.

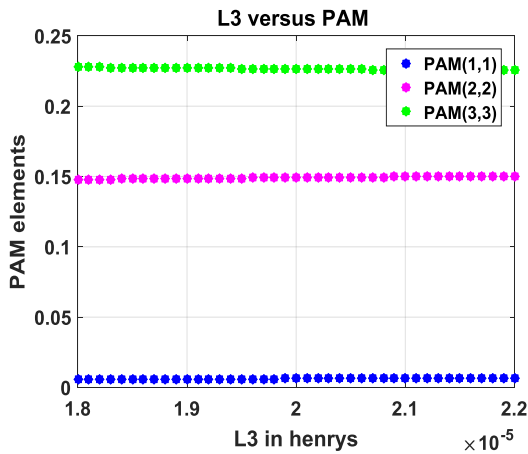


Fig. 15. L_3 vs PM 's diagonal elements.

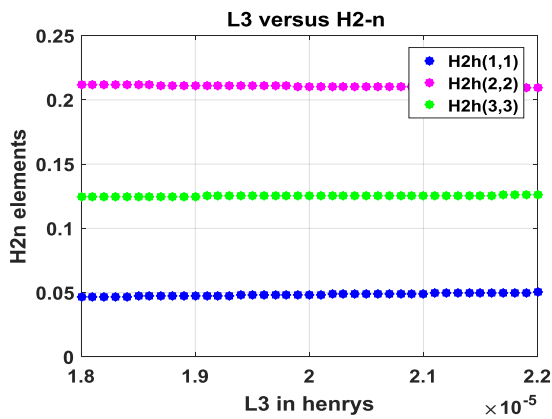


Fig. 16. L_3 vs $H_2 - n$'s diagonal elements.

Fig. 17. C_o vs $HIIA$'s diagonal elements.

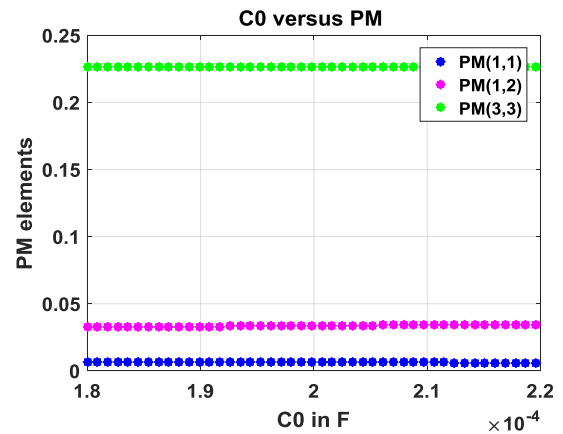


Fig. 18. C_o vs PM 's diagonal elements.

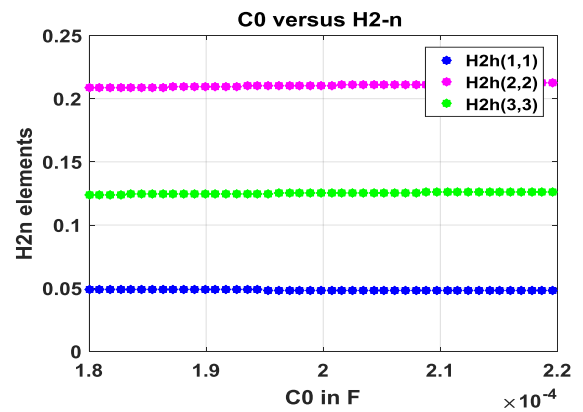
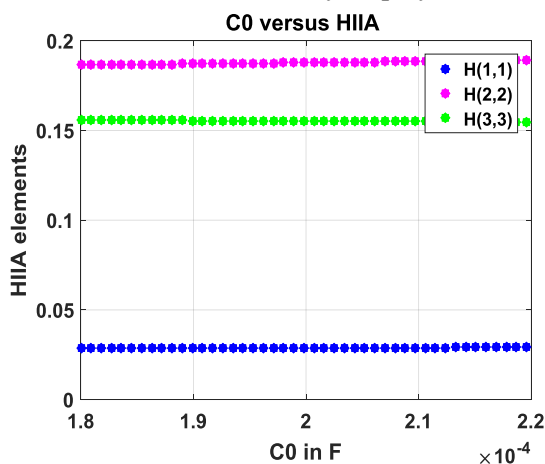


Fig. 19. C_o vs $H_2 - n$'s diagonal elements.

5.5. C_o variation in relation to interaction matrix elements:

C_o variation, which is varied by $\pm 20\%$, is taken into consideration to examine how it affects interactions. In Figs. 17-19, the effects of each parameter on the interaction measures are visually displayed.



6. Simulations and Experimental Results

Figure 20 shows the test bench, and using RT-LAB simulation software, the accuracy of the TIID converter is verified in the MATLAB environment that is connected to the OPAL4510-RT simulator. OPAL4510-RT is the name of the Hardware-in-the-Loop (HIL) testing device [24],[25]. An oscilloscope is utilized for real-time observations for digital storage (DSO) and is used to simulate the converter.

The simulated outputs V_o , I_o and duty ratios d_1, d_2 and d_3 under nominal operating conditions given in Table A1 are shown in Figs. 21 and 22 respectively. The corresponding OP4510 HIL Simulation results measured in DSO are shown in Figs. 23-25, respectively.

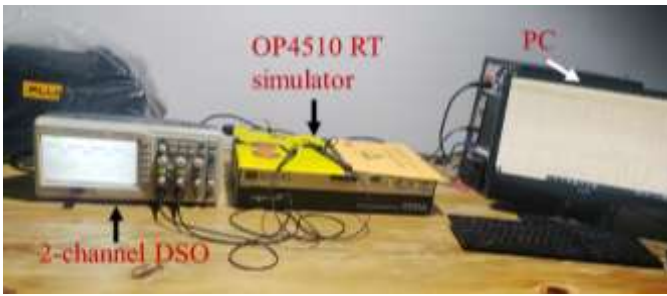


Fig. 20. OPAL4510-RT Simulator test bench

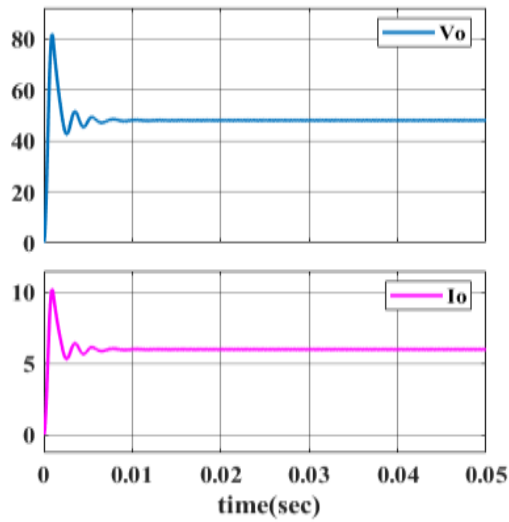


Fig.21. TIID converter's V_o , I_o

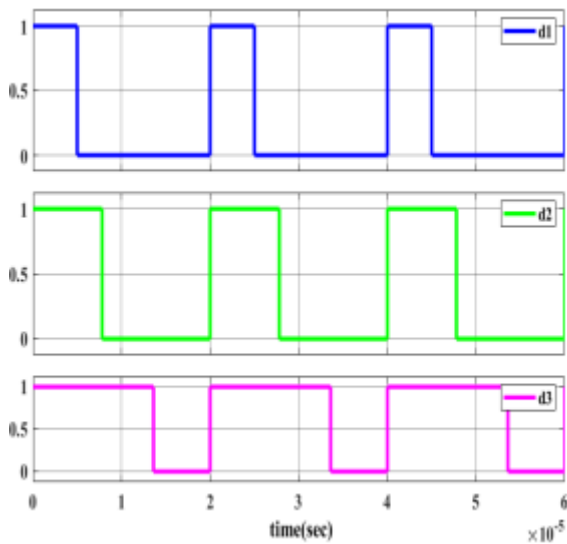


Fig.22. duty ratios of the converter

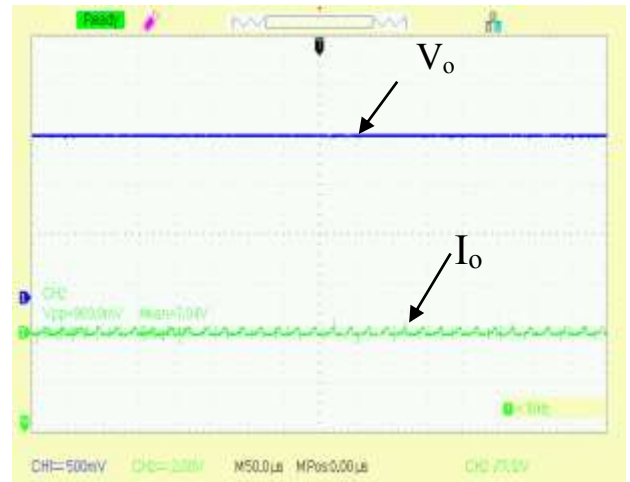


Fig.23. V_o , I_o of TIID converter

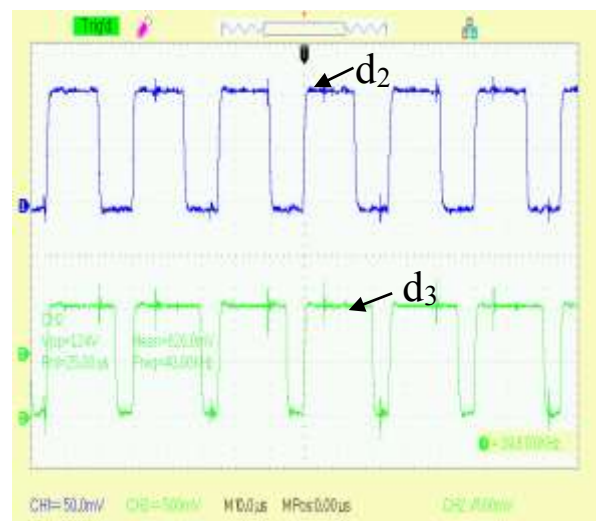


Fig.24. duty ratios d_2 , d_3 of TIID converter

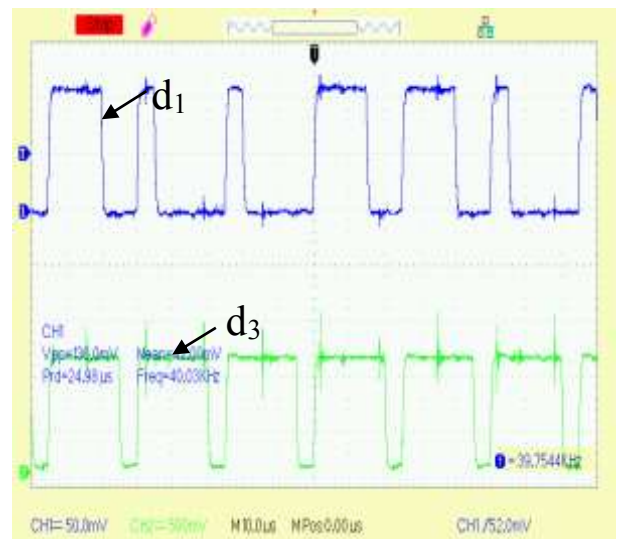


Fig.25. duty ratios d_1 , d_3 of TIID converter

7. Conclusion

The Frequency based (Gramian) interaction metrics ($H_2 - n$, $HIIA$ and PM) for a Three-Input Integrated Dc-Dc (TIID) converter were investigated and analysed. Methodologies and computational procedures are discussed. An analysis of the TIID converter's interaction measures is done using MATLAB programming. The analysis of the I/O pairing proposals offered by each measure shows that they all provide the same type of I/O pairing, which is diagonal pairing. It was found that the pairing ideas were always the same as the nominal suggestions after witnessing the interactions under different operating conditions. Plots are used to illustrate the effects of parameter changes on interaction measures. The results demonstrate that changes in the parameters have no effect on the interaction measurements. The experimental findings of the TIID converter are obtained using the Hardware In Loop (HIL) environment of the OPAL RT simulator OP4510 integrated with MALTAB.

The future scope of this work is (i) to design different diagonal controllers for TIID converter as suggested by Gramian measures, (ii) to analyse the stability of all the designed closed-loop TIID converter systems, (iii) the sensitivity analysis is to be carried out.

APPENDIX

The TIID converter operates on a 48V dc-bus regulation. Table A1 lists the specifications that are taken into consideration here. With these parameters, MATLAB calculates the TFM G of the TIID converter taking into account every mode described in section 2 and provides G as given in (5) from (A1)- (A9).

Table A1: Specifications and Parameter Values

Parameters	Value
V_{g1}, V_{g2}, V_{g3}	36V,30V,24V
V_o , Load power P_o	48V, 288W
i_{L1}, i_{L2}	2.5A,2A
L_1, L_2, L_3	150μH,250μH, 20μH

C_o	200μF
Switching frequency f_s	50KHz
$\Delta i_L, \Delta V_o$	10%, 5%

$$G_{11} = \frac{-0.3488s^4 - 2.493x10^4s^3 + 1.051x10^9s^2 + 5.608x10^{12}s + 1.796x10^{15}}{s^4 + 6195s^3 + 6.126x10^7s^2 + 1.3x10^{11}s + 2.885x10^{13}} \tag{A1}$$

$$G_{12} = \frac{0.6379s^4 + 1.293x10^5s^3 + 6.573x10^9s^2 + 2.308x10^{12}s + 6.963x10^{13}}{s^4 + 6195s^3 + 6.126x10^7s^2 + 1.3x10^{11}s + 2.885x10^{13}} \tag{A2}$$

$$G_{13} = \frac{-0.4423s^4 - 4.073x10^4s^3 + 3.755x10^8s^2 + 2.48x10^{12}s + 8.226x10^{13}}{s^4 + 6195s^3 + 6.126x10^7s^2 + 1.3x10^{11}s + 2.885x10^{13}} \tag{A3}$$

$$G_{21} = \frac{3.249x10^5s^3 + 2.093x10^9s^2 + 1.442x10^{13}s + 1.382x10^{16}}{s^4 + 6195s^3 + 6.126x10^7s^2 + 1.3x10^{11}s + 2.885x10^{13}} \tag{A4}$$

$$G_{22} = \frac{-4253s^3 - 7.506x10^8s^2 - 3.238x10^{13}s - 1.029x10^{16}}{s^4 + 6195s^3 + 6.126x10^7s^2 + 1.3x10^{11}s + 2.885x10^{13}} \tag{A5}$$

$$G_{23} = \frac{2949s^3 + 1.943x10^8s^2 - 1.899x10^{12}s - 1.215x10^{16}}{s^4 + 6195s^3 + 6.126x10^7s^2 + 1.3x10^{11}s + 2.885x10^{13}} \tag{A6}$$

$$G_{31} = \frac{4.446x10^7s^2 - 2.665x10^{12}s - 1.243x10^{16}}{s^4 + 6195s^3 + 6.126x10^7s^2 + 1.3x10^{11}s + 2.885x10^{13}} \tag{A7}$$

$$G_{32} = \frac{-2552s^3 - 4.15x10^8s^2 - 1.577x10^{13}s - 1.4x10^{15}}{s^4 + 6195s^3 + 6.126x10^7s^2 + 1.3x10^{11}s + 2.885x10^{13}} \tag{A8}$$

$$G_{33} = \frac{1.967x10^5s^3 + 1.237x10^9s^2 + 1.061x10^{13}s + 1.592x10^{16}}{s^4 + 6195s^3 + 6.126x10^7s^2 + 1.3x10^{11}s + 2.885x10^{13}} \tag{A9}$$

References

[1]H. Matsuo,W. Lin, F. Kurokawa, T. Shigemizu, and N.Watanabe, "Characteristics of the multiple-input DC-DC converter,," *IEEE Trans. Ind.Electron.*, vol. 51, no. 3, pp. 625-631, Jun. 2004.

- [2] J. Zhou, G. Nygaard and E. H. Vefring, "Adaptive decentralized control of DC-DC converter systems," 2012 7th IEEE Conference on Industrial Electronics and Applications (ICIEA), 2012, pp. 576-581.
- [3] S. Skogestad and I. Postlethwaite, "Multivariable Feedback Control: Analysis and Design," John Wiley & Sons, 1996.
- [4] D. Chen and D. E. Seborg, "Relative gain array analysis for uncertain process models," *AICHE journal*, Vol. 48 no. 2, pp. 302-310, Feb. 2002.
- [5] Conley and M. E. Salgado, "Gramian based interaction measure," in Proc. of *IEEE Int. Conference, CDC 2000*, vol. 5, pp. 5020-5022.
- [6] B. Wittenmark and M. E. Salgado, "Hankel-norm based interaction measure for input-output pairing," *IFAC World Congress*, vol. 139, pp. 429-434, Jan. 2002.
- [7] Yuan-Chuan Liu and Yaow-Ming Chen, "A Systematic Approach to Synthesizing Multi-Input DC-DC Converters," *IEEE transactions on power electronics*, vol. 24, no. 1, january 2009, pp. 116-127.
- [8] B. A. Reddy and M. Veerachary, "Gramian based digital controller design for two-input integrated DC-DC converter," *2013 International Conference on Control Communication and Computing (ICCC)*, 2013, pp. 335-340, doi: 10.1109/ICCC.2013.6731675
- [9] B. A. Reddy and M. Veerachary, "Hankel-norm based interaction analysis and digital controller design for two-input integrated DC-DC converter," *2013 Annual IEEE India Conference (INDICON)*, 2013, pp. 1-6, doi: 10.1109/INDCON.2013.6725943
- [10] P. Thota, A. R. Bhimavarapu and V V S Bhaskara Reddy Chintapalli, "Selection of input-output pairing and control structure configuration using interaction measures for DC-DC dual input zeta-SEPIC converter," *Electrica.*, November 12, 2022.
- [11] Thota, P., Bhimavarapu, A.R. and Chintapalli, V.V.S.B.R. (2022), "Participation Factor based analysis of PVSC type Multi-Input Zeta-SEPIC dc-dc converter", *COMPEL - The international journal for computation and mathematics in electrical and electronic engineering*, Vol. 41 No. 5, pp. 1727-1752. <https://doi.org/10.1108/COMPEL-10-2021-0363>
- [12] S. Upadhyaya and M. Veerachary, "Interaction Quantification in Multi-Input Multi-Output Integrated DC-DC Converters," *2021 IEEE 4th International Conference on Computing, Power and Communication Technologies (GUCON)*, 2021, pp. 1-6, doi: 10.1109/GUCON50781.2021.9573935.
- [13] Ling-Jian Ye and Zhi-huan Song, "New loop pairing criterion based on interaction and integrity considerations", *Journal of Zhejiang University: Science C* 11(5):381-393, May 2010.
- [14] Fredrik Bengtsson, Torsten Wik, "Finding feedforward configurations using gramian based interaction measures", *Modeling, Identification and Control*, Vol. 42, No. 1, 2021, pp. 27-35, ISSN 1890-1328.
- [15] Guo, X.; Shirkhani, M.; Ahmed, E.M, "Machine-Learning-Based Improved Smith Predictive Control for MIMO Processes", *Mathematics* **2022**, 10, 3696. <https://doi.org/10.3390/math10193696>.
- [16] Sumit Kumar Pandey, Jayati Dey, Subrata Banerjee, "Generalized discrete decoupling and control of MIMO systems", *Asian Journal of Control*, Volume 24, Issue 6, November 2022, Pages 3326-3344.
- [17] A. Gupta, R. Ayyanar and S. Chakraborty, "Novel Electric Vehicle Traction Architecture With 48 V Battery and Multi-Input, High Conversion Ratio Converter for High and Variable DC-Link Voltage," in *IEEE Open Journal of Vehicular Technology*, vol. 2, pp. 448-470, 2021, doi: 10.1109/OJVT.2021.3132281.
- [18] I. Alhamrouni, M. Salem, Y. Zahraoui, B. Ismail, A. Jusoh, and T. Sutikno, "Multi-input interleaved DC-DC converter for hybrid renewable energy applications," *Bulletin of Electrical Engineering and Informatics*, vol. 11, no. 3, pp. 1765-1778, Jun. 2022, doi: 10.11591/eei.v11i3.3779.
- [19] B. R. Ravada, N. R. Tummuru and B. N. L. Ande, "Photovoltaic-Wind and Hybrid Energy Storage Integrated Multi-Source Converter Configuration for DC Microgrid Applications," in *IEEE Transactions on Sustainable Energy*, vol. 12, no. 1, pp. 83-91.

- [20] V. Häberle, M. W. Fisher, E. Prieto-Araujo and F. Dörfler, "Control Design of Dynamic Virtual Power Plants: An Adaptive Divide-and-Conquer Approach," in *IEEE Transactions on Power Systems*, vol. 37, no. 5, pp. 4040-4053, Sept. 2022, doi: 10.1109/TPWRS.2021.3139775.
- [21] E. Sánchez-Sánchez, D. Groß, E. Prieto-Araujo, F. Dörfler and O. Gomis-Bellmunt, "Optimal Multivariable MMC Energy-Based Control for DC Voltage Regulation in HVDC Applications," in *IEEE Transactions on Power Delivery*, vol. 35, no. 2, pp. 999-1009, April 2020, doi: 10.1109/TPWRD.2019.2933771.
- [22] A. Khodamoradi, G. Liu and P. Mattavelli, "Online Controller Tuning for DC Microgrid Power Converters With the Ability to Track Maximum Allowable Bandwidth," in *IEEE Transactions on Industrial Electronics*, vol. 69, no. 2, pp. 1888-1897, Feb. 2022, doi: 10.1109/TIE.2021.3057009.
- [23] M. Manogna, B. A. Reddy and K. Padma, "Modeling of a Three-Input Fourth-Order Integrated DC-DC Converter," *2022 International Conference on Smart and Sustainable Technologies in Energy and Power Sectors (SSTEPS)*, Mahendragarh, India, 2022, pp. 83-88, doi: 10.1109/SSTEPS57475.2022.00032.
- [24] Santosh Kumar Reddy, P.L., Obulesu, Y.P. Design and Development of a New Transformerless Multi-port DC-DC Boost Converter. *J. Electr. Eng. Technol.* (2022). <https://doi.org/10.1007/s42835-022-01145-9>.
- [25] Anjali Atul Bhandakkar and Lini Mathew Dr. 2018 IOP Conf. Ser.: Mater. Sci. Eng. 331 012028.